



## Analytical assessment of sodium ISFET based sensors for sweat analysis

Meritxell Rovira<sup>a</sup>, Celine Lafaye<sup>b</sup>, Shu Wang<sup>c</sup>, Cesar Fernandez-Sanchez<sup>a,d</sup>,  
Mathieu Saubade<sup>b,e</sup>, Shih-Chii Liu<sup>c</sup>, Cecilia Jimenez-Jorquera<sup>a,\*</sup>

<sup>a</sup> Instituto de Microelectrónica de Barcelona (IMB-CNM), CSIC, Barcelona, Spain

<sup>b</sup> Swiss Olympic Medical Center, Lausanne University Hospital, Lausanne, Switzerland

<sup>c</sup> Sensors Group, Institute of Neuroinformatics, University of Zurich and ETH Zurich, Zurich, Switzerland

<sup>d</sup> CIBER de Bioingeniería, Biomateriales y Nanomedicina (CIBER-BBN), Barcelona, Spain

<sup>e</sup> Center for Primary Care and Public Health (Unisanté), Lausanne University Hospital, Lausanne, Switzerland

### ARTICLE INFO

#### Keywords:

Sodium ISFETs  
Sensor characterization  
Sweat analysis

### ABSTRACT

Body thermoregulation during exercise induces sweating with the consequent loss of water, electrolytes and other compounds. The use of sweat for bioanalytical purposes has recently widespread because it is an easily accessible biofluid that can be noninvasively collected and/or directly monitored using wearable devices. Different sweat biomarkers can be monitored as indicators of the physiological status of an individual. The concentration of sweat Na<sup>+</sup> electrolyte provides information about dehydration or hyponatremia events. Among the different sensor technologies applied for Na<sup>+</sup> ion detection in sweat, ion-sensitive field-effect transistors (ISFETs) show superior features in terms miniaturization, key for working with the low volumes of sweat available, robustness, scalability and reproducibility. They also offer fast response and low impedance output signal. This work reports an in-depth study that thoroughly assesses the potential of ISFET sensors for sweat Na<sup>+</sup> analysis. Results show a reproducible sensitivity of  $60.7 \pm 0.5 \text{ mV} (-\text{Log } a_{\text{Na}})^{-1}$ , high repeatability, and lifetime up to one month. Sensor reliability is demonstrated by analysing 20 sweat samples and results are compared with the ones provided with the standard ion chromatography technique (IC). The statistical analysis demonstrates that Na<sup>+</sup> concentrations estimated with the ISFET sensor and IC are in good agreement showing a relative error of up to 20%. Results demonstrate that the sensor presented in this work can potentially be used for the continuous monitoring of Na<sup>+</sup> changes in sweat during exercise.

### 1. Introduction

Although sweat composition has been under study for decades [1], its potential as a biological sample to detect biomarkers related to physical conditions has not yet been fully exploited. The wealth of biomarkers present in eccrine sweat can offer crucial information related to the metabolic dynamics of the human body, providing medical diagnosis from both physical status such as dehydration [2] and diseases such as cystic fibrosis [3] and kidney disorders [4].

Early studies in sweat composition showed the importance of the loss of chloride during continued sweating [5]. The work by Baker et al. [6] shows that as sweat flows through the duct, Na<sup>+</sup>, K<sup>+</sup> and Cl<sup>-</sup> are passively reabsorbed. As sweat rate increases, the rate of Na<sup>+</sup> and Cl<sup>-</sup> secretion in

sweat increases proportionally more than the rate of Na<sup>+</sup> and Cl<sup>-</sup> reabsorption, therefore leading to higher final sweat Na<sup>+</sup> and Cl<sup>-</sup> concentrations. Consequently, the NaCl loss may be significant during exercise performance. Whole body sweat Na<sup>+</sup> concentration has been demonstrated to be highly dependent on the heat acclimatization status and the energy expenditure.

The normal concentration of Na<sup>+</sup> in sweat ranges from 10 to 100 mM [6]. However, it is well-known that sweat rate and sweat electrolyte concentrations can vary significantly as a result of many within- and between-athlete factors [7]. The huge inter-individual variability in sweat rate and sweat sodium concentration leads to the need of personalized models to estimate the water and sodium losses and to provide fluid/electrolyte replacement strategies for avoiding

*Abbreviations:* CMOS, Complementary metal-oxide semiconductor; DOS, Bis(2-ethylhexyl)sebacate; CI, Confidence interval; FIM, Fixed interference method; IC, Ion chromatography; ISE, Ion-selective electrode; ISFET, Ion-sensitive field-effect transistor; LOA, Limit of agreement; LOD, Limit of detection; PMMA, Poly(methyl metacrylate); SOI, Silicon on insulator; TRIS, Tris(hydroxymethyl)aminomethane; SD, Standard deviation.

\* Corresponding author.

E-mail address: [cecilia.jimenez@csic.es](mailto:cecilia.jimenez@csic.es) (C. Jimenez-Jorquera).

<https://doi.org/10.1016/j.snb.2023.134135>

Received 23 February 2023; Received in revised form 6 June 2023; Accepted 10 June 2023

Available online 12 June 2023

0925-4005/© 2023 The Authors. Published by Elsevier B.V. This is an open access article under the CC BY-NC-ND license (<http://creativecommons.org/licenses/by-nc-nd/4.0/>).

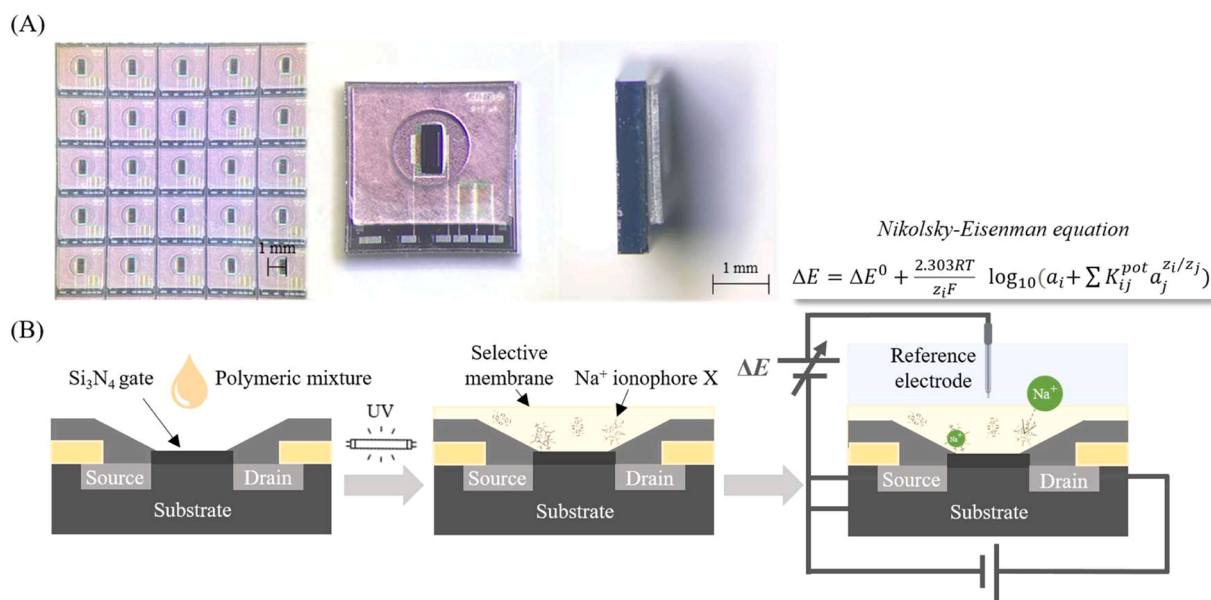


Fig. 1. (A) Pictures of the ISFETs wafer and the front and side views of an individual ISFET chip. (B) Schematic of the membrane deposition procedure and the detection mechanism.

dehydration or hyponatremia [8]. A previous study reported that 20% of marathoners in a race would need special sodium intake recommendations due to their high sweat salt losses [9]. Furthermore, oral supplements have been observed to be effective in reducing body weight loss and increasing serum electrolyte concentration [10].

Different strategies to monitor electrolyte losses have been assessed during the practice of exercise [11]. Quantitative analysis of this loss currently relies on collection of sweat from skin using different types of absorbent pads. Sweat samples are taken and analysed in centralized laboratories using benchtop equipment that is bulky, expensive and managed by highly skilled technicians. Although sweat is an accessible biofluid, its production is very low and small volume samples can be collected for analysis in a short period of time. Thus, sweat rates during exercise performance usually range  $1\text{--}2 \mu\text{L} (\text{min}\cdot\text{cm}^2)^{-1}$  in regions such as the back, forehead or forearm [12]. Deployment of compact analytical tools for in-situ sweat monitoring has been the subject of a wide variety of recent studies. The real-time monitoring represents one of the major challenges in sweat analysis, as the sensors should be able to work with few microliters of sweat and provide very rapid results. This means that the time from sample collection to sensor response should be very short and for that an optimization of the sized and geometries of sample collection areas, fluid management as well as sensor and reference electrode separations must be studied in detail. Recent advances in materials science, microfabrication and microfluidics have enabled the emergence of wearable devices placed directly on the skin and able to perform sweat collection, sampling, and sweat analysis in real time [13]. However, only few wearable electrochemical systems have been in-depth compared with a standard technique [14–17]. The complexity of the sweat matrix makes achieving accurate and high-quality quantitative measurements another challenge to be faced.

Among the different technologies that have been assessed for Na<sup>+</sup> monitoring in sweat, wearable potentiometric sensors based on ion-selective electrodes (ISEs) have demonstrated great potential in physiological and clinical applications due to their rapid response and reduced required instrumentation [18]. The signal acquisition at close-to-zero current conditions enables recording in a very straightforward manner any ion content change that occurs at the interface between the sample and the ion-selective membrane [19]. Some of the ISEs advantages are that the size can be scaled down, and that they can be printed on flexible substrates and/or implemented in fluidic systems

[20]. However, ion-sensitive field-effect transistors (ISFETs) could be an excellent alternative showing additional features such as the following. These devices are robust, scalable and reproducible, offer fast response and low impedance output signal. They are small in size and compatible with complementary metal-oxide semiconductor technology (CMOS) processes, thus enabling the integration of the electronics together with the sensor on the same chip, and the production of multi-parametric sensors at low fabrication costs [21,22]. Their small size enables working with very low sample volumes, this being key for real-time monitoring applications. As an example of wearable applications, Nakata et al., developed a wearable device with a pH ISFET and a temperature sensor integrated in a flexible substrate [23]. Zhang et al., showed the feasibility of integrating an array of ISFETs into a wearable platform to monitor multiple metabolite and parameters such as pH, Na<sup>+</sup>, K<sup>+</sup> and Ca<sup>2+</sup> concentrations [24]. Moreover, Garcia-Cordero et al., demonstrated that pH, Na<sup>+</sup>, and K<sup>+</sup> ISFETs can be used with 3D integrated CMOS compatible microfluidics for sweat collection and passive sweat driving to the ISFET sensor areas [25].

Although ISFETs have been reported in sweat wearable devices, an in-depth study that thoroughly assesses the potential of these type of sensors for sweat analysis has not been reported. In this paper, an extensive characterization of a Na<sup>+</sup> ISFET is presented, including a study of the sensor response characteristics in sweat media, and the possible chemical interferences present in this biological fluid. The final analytical assessment of Na<sup>+</sup> ISFETs is performed with the measurement of real sweat samples in a flow system designed for low volume samples and the comparison of the sensor analytical data with that of the ion chromatography reference method.

## 2. Experimental section

### 2.1. Reagents and solutions

All reagents were of high purity, analytical grade or equivalent and were purchased from Sigma-Aldrich, unless stated otherwise. All solutions were prepared using deionized water.

An artificial sweat solution was prepared based on the recipe reported in [26]. The solution contained electrolytes, amino acids, nitrogenous substances, and vitamins as indicated in Table S1 in the Supporting Information (SI).

The artificial sweat solution was spiked with tris(hydroxymethyl)aminomethan (TRIS), NaCl and KNO<sub>3</sub> at five different concentration levels ranging 10–160 mM NaCl, 2–32 mM KNO<sub>3</sub> and pH 4–8 for the characterization and calibration of the sensors before sample analysis.

## 2.2. Sweat sample collection and analysis

Sweat samples were collected from the same subject during indoor cycling sessions at the *Swiss Olympic Medical Center of the Lausanne University Hospital*. The sessions were part of a study approved in September, the 13th, 2019 by the ethical commission of the Canton of Vaud, Switzerland (Protocol No. 2019\_01235), and therefore they were performed in accordance with the ethical standards laid down in the 1964 Declaration of Helsinki. The subject was fully informed of the nature and risks of the study, and was free to withdraw at any stage of the study.

Each session was divided into 3 phases with different effort levels, each one lasting 20 min. Medical gauzes were used to collect the sweat directly from the skin of the subject's upper chest. Gauzes were covered with PET films to avoid evaporation and removed after each phase in order to extract the sweat from the gauze using a syringe. Each sweat sample was divided in two aliquots, one analysed with the reference method and the other one with the ISFET sensor. Samples were stored in sealed tubes at –20°C before analysis.

For analysis of the sweat samples, ion chromatography (IC) (940 Professional IC Vario, Metrohm, Switzerland) was used as the reference method. The samples were first filtered to remove particulate and organic matter and then diluted with water in order to get a sample conductivity of 500 µS. For both in the IC and the ISFETs analyses, the 20 samples were analysed consecutively on the same day, under the same experimental conditions.

## 2.3. Devices and equipment

ISFET chips were fabricated at the Clean Room of the IMB-CNM Institute of Microelectronics of Barcelona according to standard photolithographic techniques [27]. Each chip size was 3 × 3 mm<sup>2</sup>. The chips were fabricated on SOI (silicon on insulator) wafers to electrically isolate the ISFET from the substrate and Si<sub>3</sub>N<sub>4</sub> gate. The novelty of the fabrication in comparison with the existing technology [27] is the encapsulating layer to define a window for the membrane deposition and protecting the chip surface (Fig. 1A). This layer was deposited on wafer level making the fabrication process simpler and more reproducible. The fabrication is described in the SI.

Even though sweat is an easily accessible biofluid, the volume that can be collected in a reasonable time is low (<0.5 mL). For that reason, the flow system described in 2.4.1 (Fig. S1AB, SI) was designed. This assembly was fabricated with poly(methyl metacrylate) (PMMA) using a CO<sub>2</sub>-laser system (Epilog Mini 24, Epilog Laser, United States). It was formed by 60 mm × 30 mm PMMA layers of different thickness. The different layers were assembled with screws and O-rings were used to avoid fluid leakage. A 500 µm width channel and a well aligned with the gate of the ISFET were defined. The inner volume of the flow cell was 50 µL (sum of the channel volume, from inlet to outlet, and the volume required to fill the ISFET and the reference electrode reservoirs).

The potentiometric measurements were performed with a portable homemade multi-ISFET meter fabricated at the IMB-CNM [28]. The ISFET measurement was carried out by applying 100 µA and 0.5 V between the drain and the source, and recording the ISFET gate potential (in mV). The visualization of the results and their treatment was carried out using a laptop connected by USB to the multi-ISFET meter and by employing a virtual instrument programmed with LabView 2013 (National Instruments, Austin, USA).

An Orion 90-02-00 double junction Ag/AgCl reference electrode (Thermo Fisher Scientific Inc., Waltham, MA, USA) with 3 M KNO<sub>3</sub> solution in its outer chamber was employed to test the sensors in batch. A

Dri-Ref Reference Electrode of 5 mm diameter (World Precision Instruments, Sarasota, Florida, USA) was used in tests with the flow system.

## 2.4. Sensor fabrication

The Na<sup>+</sup> ISFET sensors were fabricated by modifying the pH ISFET gate with polymeric membranes. The membranes were prepared from Ebecryl® photocurable polymers (Allnex Resins, Germany GmbH). The ionophore used was 4-tert-butylcalix [4] arenetetraacetic acid tetraethyl ester (Ionophore X). Bis(2-ethylhexyl)sebacate (DOS) was used as plasticizer and potassium tetrakis(4-chlorophenyl)borate (KtClPhB) as lipophilic anionic additive. Membrane composition and preparation details has been presented elsewhere [29]. The deposition of the membrane mixture on the ISFET's gate is described in the SI. In Fig. 1B the mechanism of detection of the ISFETs with selective membranes is outlined. The change of potential at the gate of the ISFET due to the presence of the analyte is described by the Nikolsky-Eisenman equation [30] (see Fig. 1B), which incorporates the interferent contributions to the potential defined by Nernst equation.

## 2.5. Sensor characterization methodologies

Initially, the analytical performance of the Na<sup>+</sup> ISFETs was done with an Orion Ag/AgCl reference electrode in batch conditions. Next, they were evaluated in flow conditions with a Dri-Ref reference electrode and real samples were measured. In all cases, sensors were previously conditioned in the corresponding media (NaCl 10<sup>-3</sup> M) to achieve stable potentials in the corresponding media.

## 2.6. Batch methods

To determine the response characteristics of ISFETs (sensitivity, linear range, limit of detection (LOD) and minimum step change), calibrations were performed by adding certain volumes of 10<sup>-4</sup>, 10<sup>-2</sup>, 10<sup>-1</sup>, and 1 M NaCl standard solutions to 50 mL of water every 1.5–2 min under stirring. The sensor lifetime and working stability were studied by performing periodic calibrations during more than one month (15 calibrations) in artificial sweat solutions.

The hysteresis effect of the different ISFETs was evaluated doing a double calibration by first increasing and then decreasing NaCl concentrations. Five separate solutions of 10, 20, 40, 80, and 160 mM NaCl were used, and the sensors were successively changed from one to another every 60 s

The influence of the solution pH on the Na<sup>+</sup> ISFET response was tested by immersing the sensors in five solutions containing 10 mM NaCl at pH 4, 5, 6, 7, and 8 (pH corrected with TRIS and HCl). The sensors were sequentially immersed in solutions from higher to lower pH in triplicate.

The most interfering ion for Na<sup>+</sup> ISFET is K<sup>+</sup>, so its selectivity was evaluated. We used the fixed interference method (FIM) fixing the K<sup>+</sup> ion concentration at 1 mM and 32 mM (minimum and maximum concentration values in the range of K<sup>+</sup> in sweat) and varying Na<sup>+</sup> concentration from 10<sup>-7</sup> M to 160 mM by adding small volumes of NaCl stock solutions to the solutions under stirring. The selectivity coefficient values (K<sub>Na,K</sub><sup>pot</sup>) could be obtained from the LODs.

To test the selectivity of Na<sup>+</sup> membrane against other components present in sweat, six solutions containing 10 mM NaCl and possible interferents were prepared (defined in SI). Three sensors were immersed first in a 10 mM NaCl solution and then, they were successively dipped for 1 min in the six solutions. Finally, they were immersed in a 20 mM NaCl to test their sensitivity to Na<sup>+</sup>. In another study, ten Na<sup>+</sup> ISFETs were calibrated in the presence of compounds corresponding to each family (Table S1, SI).

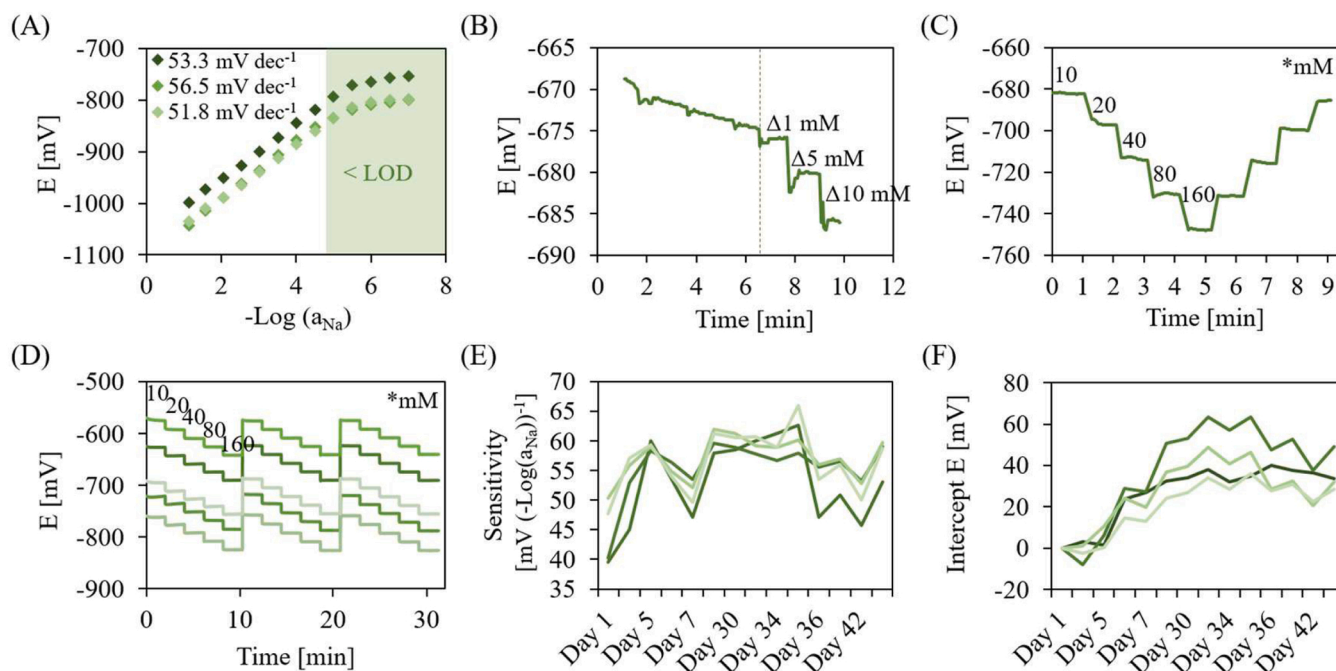


**Fig. 2.** (A) Calibration plots of three  $\text{Na}^+$  ISFETs over the whole concentration range. (B) Recording of the potential changes when adding increasing volumes of NaCl standard solutions. The dashed line indicates the minimum step change that can be detected with Nernstian slope. (C) Hysteresis recording for calibrations in the sweat range from 10 mM to 160 mM  $\text{Na}^+$ . (D) Recordings of three consecutive calibrations at five concentration steps to study repeatability and reproducibility. Sensitivity (E) and intercept potential (F) of four ISFETs calibrated periodically during a period of 43 days.

## 2.7. Flow system methods

The analysis of sweat samples was performed in the flow system (Fig. S1AB, SI). A first characterization of the system was performed with artificial sweat solutions containing different NaCl concentrations into the system. The flow rate was set at  $8.3 \mu\text{L s}^{-1}$  (5 rpm) during both the characterization and the sample analysis. The contamination between calibration solutions and samples was avoided by injecting water and air in between solutions for 30 s and 15 s, respectively. A Dri-Ref compact reference electrode was used for these studies. The reversibility of the signal was evaluated by pumping artificial sweat solution spiked with 1 mM NaCl before and after calibration solutions and sweat samples.

Sweat samples were left to reach room temperature before the analysis. Then, they were injected in the flow system in order to fill the PMMA cell channel. The flow was stopped for 120 s to ensure the recording of steady-state potential values.

## 3. Results and discussion

$\text{Na}^+$  ISFETs were first characterized under batch conditions to assess their analytical performance for sweat  $\text{Na}^+$  analysis. Their response was also evaluated in a flow system and validated with sweat samples.

### 3.1. Sensor batch characterization

The performance of the ISFETs was studied in a wide range of NaCl concentrations ( $10^{-7} \text{ M} - 1 \text{ M}$ ) without presence of interfering ions. The sensors displayed a LOD of  $9.4 \times 10^{-6} \pm 4.9 \times 10^{-6} \text{ M}$  and a reproducible Nernstian slope of  $53.9 \pm 2.4 \text{ mV } (-\text{Log } a_{\text{Na}})^{-1}$  in a linear range of  $3.2 \times 10^{-5} \text{ M} - 1 \text{ M}$  NaCl as shown in Fig. 2A. This range includes the physiological  $\text{Na}^+$  concentrations expected in sweat.

The minimum step change in concentration that could be differentiated from noise was determined with jumps in concentration ranging from 0.01 mM to 10 mM. From the results it was concluded that differences up to  $\Delta 1 \text{ mM}$ , corresponding to 1.07 mV, could be

quantitatively detected (Fig. 2B).

To study the reversibility of the ISFETs they were calibrated with NaCl solutions, from low to high and from high to low concentrations (Fig. 2C). The signal difference between the same concentration levels was  $2.1 \pm 1.0 \text{ mV}$ . This difference may be due to the ions trapped in the membranes. In real applications this memory effect may be negligible.

The repeatability for the same ISFET sensor was quantified. For that, five ISFETs were immersed in a water solution whose  $\text{Na}^+$  concentration was increased from 10 mM to 160 mM. The sensors were calibrated three times. In Fig. 2D these calibration curves are depicted and in Table S2 in SI the values of slope and intercept for each calibration and ISFET are detailed. Although the repeatability was high for each ISFET – sensitivity's average standard deviation of  $2.3 \pm 1.0 \text{ mV } (-\text{Log } a_{\text{Na}})^{-1}$  and intercept average standard deviation of  $3.1 \pm 1.3 \text{ mV}$  – results were better for the 2nd and 3rd calibration replicates – sensitivity average SD  $0.6 \pm 0.5 \text{ mV } (-\text{Log } a_{\text{Na}})^{-1}$  and intercept average SD  $0.6 \pm 0.4 \text{ mV}$  – indicating that the sensor requires a certain conditioning before calibration.

From this study, the reproducibility between different sensors was assessed. The mean sensitivity value obtained for the five ISFETs tested was  $60.7 \pm 0.5 \text{ mV } (-\text{Log } a_{\text{Na}})^{-1}$ , using the values of the third calibration. The mean value of the intercept was  $-797.4 \pm 74.7 \text{ mV}$ . This value is indicative of the  $V_{\text{th}}$  of ISFET and it is within the technological parameters already defined for these ISFETs [31,32]. In previous works using  $\text{Na}^+$  ISFET sensors for sweat analysis, values ranging from 55 to 62  $\text{mV } (-\text{Log } a_{\text{Na}})^{-1}$  were found [17,24,25,33]. However, they did not show a full analytical characterisation of the devices in terms of the other operational parameters presented in this work (LOD, minimum concentration change detectable, working stability, etc.). From our experiments, it could be concluded that the ISFETs showed reproducible Nernstian responses in the  $\text{Na}^+$  physiological concentration range in sweat.

A study was performed in order to evaluate the lifetime of  $\text{Na}^+$  ISFETs and its working stability. For that, four ISFETs were periodically calibrated in artificial sweat solution over a period of more than one month (Fig. 2E and F). As it has been extensively reported [34,35], the

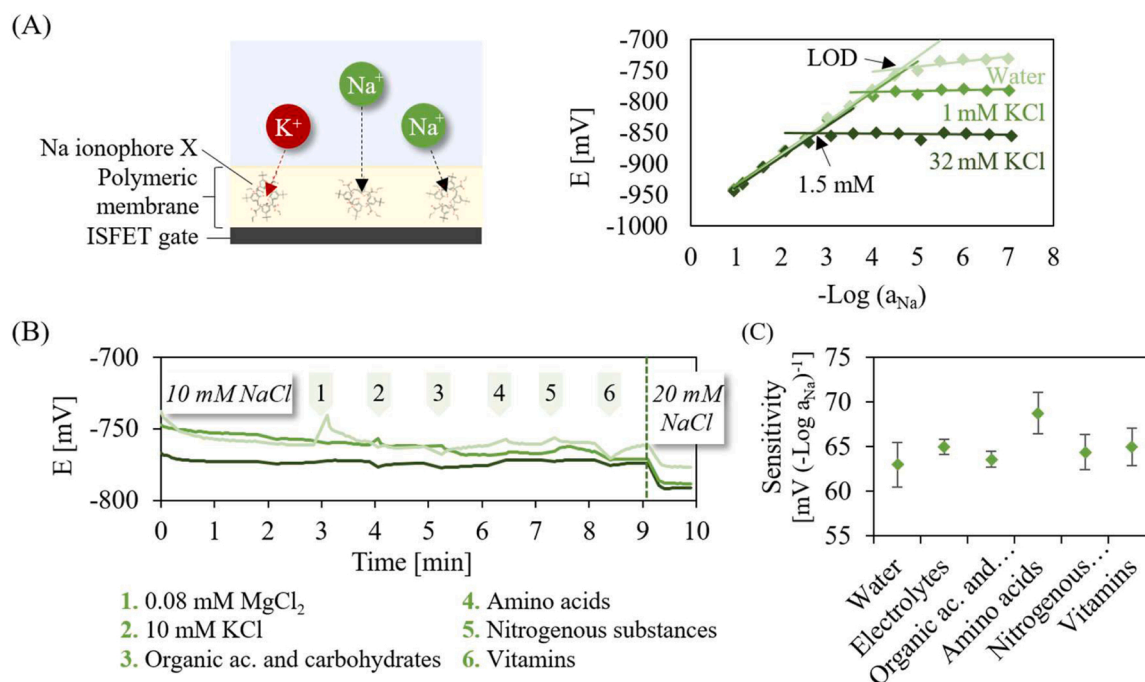


**Fig. 3.** (A) Picture of interactions between Na<sup>+</sup> and K<sup>+</sup> ions in Na<sup>+</sup> ion-selective membrane (left), and calibration plots of a Na<sup>+</sup> ISFET in deionized water and in 1 mM and 32 mM KCl solutions. (B) Recording of the potential of three Na<sup>+</sup> ISFETs in presence of potentially interfering components (grouped by families) present in human sweat. (C) Sensitivity of five Na<sup>+</sup> ISFETs to NaCl changes in different matrices.

conditioning step before the use of ion-selective potentiometric devices was critical. At first, the ISFETs were stored dry, and they were just conditioned in a 1 mM NaCl solution for 30 min before the first calibration. Apparently, it was not enough time since lower sensitivities were obtained on the first day (Fig. 2E). The maximum sensitivity could have been achieved being immersed for at least 1 h in the NaCl solution before use. For subsequent calibrations, they were stored in a 1 mM NaCl solution to ensure a stable and reproducible sensitivity value. Excluding the first-day calibration, the standard deviation of the mean sensitivity values between days was  $4.1 \pm 1.8$  mV  $(-\text{Log } a_{\text{Na}})^{-1}$ . The intercept of the calibration curves showed a similar trend for all ISFETs (Fig. 2F). Until the thirtieth day, the intercept steadily increased day after day. Later, it stabilized and then it decreased again. However, the variation of the intercept estimated considering the 15 consecutive calibrations was  $35.8 \pm 9.2$  mV on average, which is in accordance with the sensor temporal drift [36].

The pH effect on the sensor was evaluated. The potential recorded from the ISFETs in solutions containing 10 mM NaCl at the physiological range of 4–8 pH units remained almost constant (Fig. S2, SI). The standard deviation of the potential values recorded with the four ISFETs was between 0.8 and 3.5 mV.

Although the most abundant electrolytes in sweat are Na<sup>+</sup> and Cl<sup>-</sup>, some other compounds that could interfere with Na<sup>+</sup> ISFET measurements are present. For this reason, the selectivity of Na<sup>+</sup> ISFETs to other analytes was assessed. The major component in sweat that could interfere with the Na<sup>+</sup> measurement is K<sup>+</sup>. The selectivity against K<sup>+</sup> was evaluated by means of the fixed interference method. For that, the response of five Na<sup>+</sup> ISFETs was recorded under increasing concentrations of the primary ion (Na<sup>+</sup>), and in a fixed concentration interfering ion (K<sup>+</sup>). From these recordings, the selectivity coefficient,  $K_{\text{Na,K}}^{\text{pot}}$ , which defines the ability of the sensor to distinguish Na<sup>+</sup> from K<sup>+</sup>, was extracted. The smaller the value of  $K_{\text{Na,K}}^{\text{pot}}$  the greater the sensor's preference for Na<sup>+</sup>. In Fig. 3A, three calibration curves are depicted: a calibration in deionized water and two in solutions with fixed KCl concentrations. The average  $K_{\text{Na,K}}^{\text{pot}}$  in a 1 mM KCl solution was 0.0899

$\pm 0.0065$ , and in a 32 mM KCl solution was  $0.0492 \pm 0.0029$ . To define the ISFET's behaviour, the average of both values (0.0695) was used in the Nikolsky-Eisenman equation. As shown, the interference from K<sup>+</sup> ions to the response of Na<sup>+</sup> ISFETs was relatively high at concentrations of potassium above 1 mM. However, due to the 10X higher concentration of Na<sup>+</sup> over K<sup>+</sup> in sweat, this interference should not affect the measurement. This means that Na<sup>+</sup> ion concentrations that are above 1.5 mM could be detected even in solutions with 32 mM K<sup>+</sup>, value that is below the Na<sup>+</sup> physiological concentration in sweat.

In order to identify potential interferents from the different components of sweat, these interferents were added to different solutions containing 10 mM NaCl. Three ISFETs were immersed in these 10 mM NaCl solutions and finally in a 20 mM NaCl solution to check that the sensor responded to the target analyte with Nernstian sensitivity. The recordings of the test are plotted in Fig. 3B. The average potential differences between each interferent solution and the 10 mM solution without interferents were  $0.03 \pm 2.90$ ,  $-1.93 \pm 1.96$ ,  $-3.97 \pm 5.28$ ,  $-0.97 \pm 6.84$ ,  $-1.50 \pm 5.14$ ,  $-4.40 \pm 7.62$  mV for solutions 1–6, respectively. All contain the 0 in its confidence range, so they show no bias. On the other hand, the maximum difference observed would still correspond to less than a 10% of the measured concentration. Finally, the Nernstian behaviour of the sensors was verified in a 20 mM NaCl solution, where they showed sensitivities of  $55.70 \pm 3.36$  mV  $(-\text{Log } a_{\text{Na}})^{-1}$ .

An extensive test of the sweat matrix effects on the ISFET response was performed by calibrating ten sensors simultaneously in six background solutions containing different families of components present in sweat (Table S1, SI). Fig. 3C shows the results. The sensitivity to Na<sup>+</sup> in the different solutions was compared with the one in water using the paired samples t-test ( $\alpha = 0.05$ ). The values obtained in the different solutions were not statistically comparable to the ones in water, except for the organic acids and carbohydrates ( $t_{\text{calc}} 0.77 < t_{\text{tab}} 2.26$ ). Thus, the last was the only group not included in the artificial sweat solution used in the following studies.

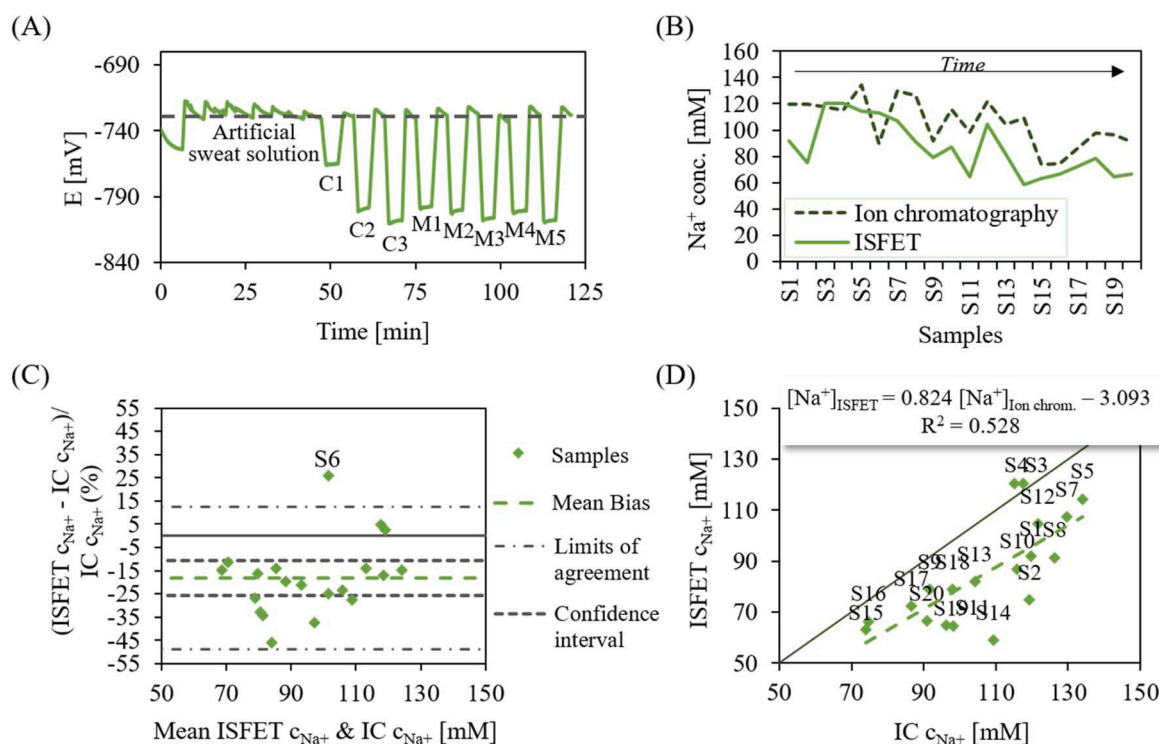


**Fig. 4.** (A) Recording of the output signal pumping artificial sweat solution, three calibration solutions and five sweat samples. (B) Sodium concentration data of 20 sweat samples, sequentially analysed with a  $\text{Na}^+$  ISFET and IC. (C) Bland-Altman plot showing the relative difference between the ISFET and IC  $\text{Na}^+$  concentration values for the 20 sweat samples, and the mean bias, the confidence interval (95%), and the limits of agreement (95%) for these values. (D) Scatter plot showing the correlation between  $\text{Na}^+$  ISFET and IC concentration values quantified at the sweat samples (identified as SX) following Pearson regression.

### 3.2. Performance of the $\text{Na}^+$ sensor under flow conditions

The performance of the  $\text{Na}^+$  ISFET sensor was also assessed under flow conditions with the aim of being able to analyse sweat samples in a faster and automatic fashion. Under flow conditions, sample renewal and sensor cleaning is highly facilitated.

In order to perform the sensor characterization under flow conditions, firstly, the stabilization of the signal or baseline was studied by injecting artificial sweat solutions to the flow cell. Fig. S1C in SI shows that the baseline achieved for the first replicate was different from the following ones. This behaviour was also observed in tests with real sweat samples. As shown, for the following replicates the baseline signal stabilized at similar potential values. Another characteristic from this response is the transient signal that appeared more pronounced for the first and second replicates. Later, the response reached a stable value in few seconds. From that, it can be concluded that the membrane needed some time for conditioning in the matrix and that the temporal drift in these conditions was negligible ( $-0.085 \text{ mV min}^{-1}$ ).

Finally, the sample renewal and sensor cleaning was evaluated by studying the reversibility of the signal. Artificial sweat solution spiked with 1 mM NaCl was pumped before and after three calibration solutions and five sweat samples (Fig. 4A). The potential recorded in the artificial sweat solution was  $-728.9 \pm 1.2 \text{ mV}$ , demonstrating good reversibility.

In order to accurately quantify the  $\text{Na}^+$  concentration present in sweat samples, the ISFET response,  $E$ , could be defined by the following contributions:

$$E = E_b - \alpha \cdot S_{Nernst} \cdot \text{Log}_{10}(a_{\text{Na}} + K_{\text{Na,K}}^{pot} \cdot a_{\text{K}}^{z_{\text{Na}}/z_{\text{K}}})$$

where:

$E_b$  is the sum of  $E^0$ , the threshold voltage change due to trapped charges in the floating gate, and the contribution of the reference electrode [22].

$S_{Nernst}$  is the ideal sensitivity given by Nernst equation. For monovalent ions and at  $25^\circ\text{C}$  its value is  $59.16 \text{ mV dec}^{-1}$ .

$\alpha$  defines the degree of deviation from the Nernstian ideal sensitivity.  $z_{\text{Na}}$  is the charge number of  $\text{Na}^+$ .

$z_{\text{K}}$  is the charge number of the interfering ion  $\text{K}^+$ .

$\alpha$  and  $E_b$  values could be obtained from the calibration of the ISFETs in artificial sweat calibration solutions.

### 3.3. Analysis of sweat samples

The final study was conducted to measure the  $\text{Na}^+$  concentration present in 20 sweat samples. The samples were previously analysed using IC as explained in Section 2.2. The  $\text{Na}^+$  concentration values achieved with both methods are depicted in Fig. 4B in the chronological order of measurement. It can be observed that, although the values were different, they followed a similar trend. It became more visible after the first six samples, when the membrane was fully conditioned. The analytical data is shown in Table S3, SI. The data values obtained from the two assays were compared with the Bland-Altman analysis. The plot in Fig. 4C shows the mean difference between the concentration values obtained with the sensor and IC, together with the 95% confidence interval around the mean and the limits of agreement (LOA). The LOAs define the interval where the 95% of the values are expected to lie. This study allowed us to remove the outliers that did not accomplished the 95% of agreement (only the sample 6 in our study). Once removed the outlier, the bias was evaluated. It appears when the 95% confidence interval does not include the 0 value. From our results, we conclude that there is a systematic bias between the methods (95% CI =  $-10.68$  to  $-25.65$ ). The existence of a bias indicates that there is a matrix effect that was not detected in the characterization of the sensors in artificial sweat. This may be due to the lipid-rich content present in the samples, that could affect the hydrophobic selective-membrane [37–39]. These substances can permeate into the polymeric membranes, changing its

**Table 1**  
State-of-the-Art (SoA) of Na<sup>+</sup> ISFETs for sweat sensing.

Concentration range [M]	Sensitivity [mV/dec]	Interference tests	Sweat samples validated	Reference method	Relative error [%]	SoA
10 <sup>-5</sup> – 1	55 <sup>a</sup>	No	5	Potentiometric <sup>b</sup>	NG <sup>c</sup>	[17]
10 <sup>-3</sup> – 10 <sup>-1</sup>	57	Yes	2	Potentiometric <sup>d</sup>	12%	[24]
10 <sup>-4</sup> – 1	57	Yes	1	Potentiometric <sup>b</sup>	4%	[33]
10 <sup>-2</sup> – 1.6·10 <sup>-1</sup>	61	Yes	20	IC	20%	This work

<sup>a</sup> The total sensitivity is the sum of Na<sup>+</sup> ISFET (55) and Ag/AgCl (55) sensitivities.

<sup>b</sup> Roche Hitachi 912 chemistry analyzer.

<sup>c</sup> NG: Not given.

<sup>d</sup> Horiba LAQUAtwin Na+ 11.

properties, and reducing the sensitivity towards Na<sup>+</sup> ions. Despite the underestimation of Na<sup>+</sup> concentration using ISFETs, the results follow similar trends (Fig. 4B).

Then, the data was represented in a scatter plot (Fig. 4D) and the linear regression between both methods was extracted. Taking the Na<sup>+</sup> concentration values from IC as reference, an average relative error of – 20.48% was calculated for the ISFETs detection (Table S3, SI). To the best of our knowledge, none of the previously reported Na<sup>+</sup> ISFETs applied for sweat sensing were thoroughly assessed with real sweat samples [17,24,33]. Table 1 compares the performance of our sensor with that of other Na<sup>+</sup> ISFETs tested in sweat. The sensitivity is similar to all of them. And although the linear range of the presented sensor is shorter, it still covers the whole Na<sup>+</sup> concentration range found in sweat. The accuracy is also slightly worse, but here the experimental conditions applied in each reported study must be considered. Using a very small number of samples, between 1 and 5, these studies do not show the full potential of the tested devices for measuring Na<sup>+</sup> target species in sweat. In our work, a representative number of samples collected at different exercise efforts and during different days on the same subject was used, which allow us to perform a more in-depth evaluation of the sensor performance and to show its potential for wearable applications. In addition, unlike previous works showing a comparative study using commercial potentiometric equipment as the reference method, the one of this work was done using IC as the reference method, which has previously shown to be the most accurate technique for this application [40,41].

Thus, ISFETs can detect relative changes in the Na<sup>+</sup> secreted in the athlete's sweat that are related to dehydration or hyponatremia. If more accurate values of Na<sup>+</sup> concentration in sweat were desired, the sensor bias could be corrected by performing a calibration before and after the samples analysis, which would enable estimating the sensor loss of sensitivity.

#### 4. Conclusions

An in-depth study of the Na<sup>+</sup> ISFET analytical behaviour was performed. Na<sup>+</sup> ISFETs exhibited near Nernstian slopes as well as limits of detection and linear ranges suitable for detecting the target biomarker in sweat. They showed a high reproducibility and response repeatability which make them suitable for performing repetitive measurements. Results of lifetime and working stability indicated that the sensitivity and baseline of the sensors were consistent over a period of at least one month. The study of the effect of the matrix composition on the sensor response revealed the necessity of calibrating the Na<sup>+</sup> ISFET sensors in a solution containing the major sweat components and including the K<sup>+</sup> concentration contribution in the Nikolsky-Eisenman equation.

A flow system set-up for the measurement of Na<sup>+</sup> concentration in low volume samples was developed. Validation with real sweat samples and comparison with IC technique showed the likely effect of the sweat lipid content on the ISFET membrane but this could easily be corrected.

The ISFETs showed good performance Na<sup>+</sup> quantification in sweat samples, being feasible their integration in compact electronic wearable devices [42,43]. As future work, the ISFETs will be integrated in a CMOS

fabricated chip for real-time, continuous monitoring of analytes on-body, allowing correction of interferences using deep learning approaches [44].

#### CRedit authorship contribution statement

**Meritxell Rovira:** Methodology, Validation, Investigation, Writing - original draft. **Celine Lafaye:** Methodology, Validation, Investigation. **Shu Wang:** Methodology, Investigation. **Cesar Fernandez-Sanchez:** Conceptualization, Supervision, Writing - review & editing. **Mathieu Saubade:** Conceptualization, Supervision. **Shih-Chii Liu:** Conceptualization, Supervision. **Cecilia Jimenez-Jorquera:** Funding acquisition, Conceptualization, Supervision, Writing – review & editing.

#### Declaration of Competing Interest

The authors declare that they have no known competing financial interests or personal relationships that could have appeared to influence the work reported in this paper.

#### Data Availability

Data will be made available on request.

#### Acknowledgements

This work was performed within the WeCare project, funded by the Swiss National Science Foundation (SNSF, Sinergia Program, Project CRSII5\_177255/1) and used the ICTS Network MICRONANOFABS supported by the Spanish Ministry of Science and Innovation. We acknowledge Anna Roldán, who actively participated in the sweat samples analysis as part of the final project of her Bachelor's degree.

#### Appendix A. Supporting information

Supplementary data associated with this article can be found in the online version at [doi:10.1016/j.snb.2023.134135](https://doi.org/10.1016/j.snb.2023.134135).

#### References

- [1] B.A. McSwiney, The composition of human perspiration (Samuel hyde memorial lecture): (section of physical medicine), *Proc. R. Soc. Med.* 27 (1934) 839–848.
- [2] S. Wang, C. Lafaye, M. Saubade, C. Besson, J.M. Margarit-Taule, V. Gremeaux, S. C. Liu, Predicting hydration status using machine learning models from physiological and sweat biomarkers during endurance exercise: a single case study, *IEEE J. Biomed. Heal. Inform.* 26 (2022) 4725, <https://doi.org/10.1109/JBHI.2022.3186150>.
- [3] B.J. Rosenstein, G.R. Cutting, The diagnosis of cystic fibrosis: a consensus statement, *J. Pediatr.* 132 (1998) 589–595, [https://doi.org/10.1016/S0022-3476\(98\)70344-0](https://doi.org/10.1016/S0022-3476(98)70344-0).
- [4] Y. Zhang, H. Guo, S.B. Kim, Y. Wu, D. Ostojich, S.H. Park, X. Wang, Z. Weng, R. Li, A.J. Bandodkar, Y. Sekine, J. Choi, S. Xu, S. Quaggin, R. Ghaffari, J.A. Rogers, Passive sweat collection and colorimetric analysis of biomarkers relevant to kidney disorders using a soft microfluidic system, *Lab Chip* 19 (2019) 1545–1555, <https://doi.org/10.1039/C9LC00103D>.
- [5] K.Neville Moss, Some effects of high air temperatures and muscular exertion upon colliers, *Proc. R. Soc. B.* 95 (1923) 181–200. <https://doi.org/10.1098/rspb.1923.0031>.

- [6] L.B. Baker, P.J.D. De Chavez, R.P. Nuccio, S.D. Brown, M.A. King, B.C. Sopena, K. A. Barnes, Explaining variation in sweat sodium concentration: Effect of individual characteristics and exercise, environmental, and dietary factors, *J. Appl. Physiol.* (2022) 1250–1259, <https://doi.org/10.1152/jappphysiol.00391.2022>.
- [7] L.B. Baker, Sweating rate and sweat sodium concentration in athletes: a review of methodology and intra/interindividual variability, *Sport. Med.* 47 (2017) 111–128, <https://doi.org/10.1007/s40279-017-0691-5>.
- [8] S.J. Montain, S.N. Cheuvront, M.N. Sawka, Exercise associated hyponatremia: quantitative analysis to understand the aetiology, *Br. J. Sports Med.* 40 (2006) 98, <https://doi.org/10.1136/BJSM.2005.018481>.
- [9] B. Lara, C. Gallo-Salazar, C. Puente, F. Areces, J.J. Salinero, J. Del Coso, Interindividual variability in sweat electrolyte concentration in marathoners, *J. Int. Soc. Sports Nutr.* 13 (2016) 1–8, <https://doi.org/10.1186/s12970-016-0141-z>.
- [10] J. Del Coso, C. González-Millán, J.J. Salinero, J. Abián-Vicén, F. Areces, M. Lledó, B. Lara, C. Gallo-Salazar, D. Ruiz-Vicente, Effects of oral salt supplementation on physical performance during a half-ironman: a randomized controlled trial, *Scand. J. Med. Sci. Sports* 26 (2016) 156–164, <https://doi.org/10.1111/SMS.12427>.
- [11] J. Choi, R. Ghaffari, L.B. Baker, J.A. Rogers, Skin-interfaced systems for sweat collection and analytics, *Sci. Adv.* 4 (2018) eaar3921, <https://doi.org/10.1126/sciadv.aar3921>.
- [12] N.A.S. Taylor, C.A. Machado-Moreira, Regional variations in transepidermal water loss, eccrine sweat gland density, sweat secretion rates and electrolyte composition in resting and exercising humans, *Extrem. Physiol. Med.* 2 (2013) 4, <https://doi.org/10.1186/2046-7648-2-4>.
- [13] T. Kaya, G. Liu, J. Ho, K. Yelamarthi, K. Miller, J. Edwards, A. Stannard, Wearable sweat sensors: background and current trends, *Electroanalysis* 31 (2019) 411–421, <https://doi.org/10.1002/elan.201800677>.
- [14] R. Vinoth, T. Nakagawa, J. Mathiyarasu, A.M.V. Mohan, Fully printed wearable microfluidic devices for high-throughput sweat sampling and multiplexed electrochemical analysis, *ACS Sens.* 6 (2021) 1174–1186, <https://doi.org/10.1021/acssensors.0c02446>.
- [15] H. Liu, Z. Gu, Q. Zhao, S. Li, X. Ding, X. Xiao, G. Xiu, Printed circuit board integrated wearable ion-selective electrode with potential treatment for highly repeatable sweat monitoring, *Sens. Actuators B Chem.* 355 (2022), 131102, <https://doi.org/10.1016/J.SNB.2021.131102>.
- [16] M. Yang, N. Sun, X. Lai, J. Wu, L. Wu, X. Zhao, L. Feng, Paper-based sandwich-structured wearable sensor with sebum filtering for continuous detection of sweat pH, *ACS Sens.* 8 (2023) 176–186, <https://doi.org/10.1021/acssensors.2c02016>.
- [17] A. Cazalé, W. Sant, F. Ginot, J.C. Launay, G. Savourey, F. Revol-Cavalier, J. M. Lagarde, D. Heinry, J. Launay, P. Temple-Boyer, Physiological stress monitoring using sodium ion potentiometric microensors for sweat analysis, *Sens. Actuators B Chem.* 225 (2016) 1–9, <https://doi.org/10.1016/J.SNB.2015.10.114>.
- [18] M. Cuartero, M. Parrilla, G.A. Crespo, Wearable potentiometric sensors for medical applications, *Page 363*, 19, *Sensors Vol. 19* (2019) 363, <https://doi.org/10.3390/S19020363>.
- [19] J. Bobacka, A. Ivaska, A. Lewenstam, Potentiometric Ion Sensors, (2008). <https://doi.org/10.1021/cr068100w>.
- [20] J. Hu, A. Stein, P. Bühlmann, Rational design of all-solid-state ion-selective electrodes and reference electrodes, *TrAC Trends Anal. Chem.* 76 (2016) 102–114, <https://doi.org/10.1016/J.TRAC.2015.11.004>.
- [21] J. Bausells, J. Carrabina, A. Errachid, A. Merlos, Ion-sensitive field-effect transistors fabricated in a commercial CMOS technology, *Sens. Actuators B Chem.* 57 (1999) 56–62, [https://doi.org/10.1016/S0925-4005\(99\)00135-5](https://doi.org/10.1016/S0925-4005(99)00135-5).
- [22] N. Moser, T.S. Lande, C. Toumazou, P. Georgiou, ISFETs in CMOS and emergent trends in instrumentation: a review, *IEEE Sens. J.* 16 (2016) 6496–6514, <https://doi.org/10.1109/JSEN.2016.2585920>.
- [23] S. Nakata, T. Arie, S. Akita, K. Takei, Wearable, flexible, and multifunctional healthcare device with an ISFET chemical sensor for simultaneous sweat pH and skin temperature monitoring, *ACS Sens.* 2 (2017) 443–448, <https://doi.org/10.1021/acssensors.7b00047>.
- [24] J. Zhang, M. Rupakula, F. Bellando, E. Garcia Cordero, J. Longo, F. Wildhaber, G. Herment, H. Guérin, A.M. Ionescu, Sweat biomarker sensor incorporating picowatt, three-dimensional extended metal gate ion sensitive field effect transistors, *ACS Sens.* 4 (2019) 2039–2047, <https://doi.org/10.1021/acssensors.9b00597>.
- [25] E. Garcia-Cordero, F. Bellando, J. Zhang, F. Wildhaber, J. Longo, H. Guérin, A. M. Ionescu, Three-dimensional integrated ultra-low-volume passive microfluidics with ion-sensitive field-effect transistors for multiparameter wearable sweat analyzers, *ACS Nano* 12 (2018) 12646–12656, <https://doi.org/10.1021/acsnano.8b07413>.
- [26] C.J. Harvey, R.F. LeBouf, A.B. Stefaniak, Formulation and stability of a novel artificial human sweat under conditions of storage and use, *Toxicol. Vitro* 24 (2010) 1790–1796, <https://doi.org/10.1016/j.tiv.2010.06.016>.
- [27] C. Jimenez-Jorquera, J. Orozco, A. Baldi, ISFET based microensors for environmental monitoring, *Sensors* 10 (2010) 61–83, <https://doi.org/10.3390/s10010061>.
- [28] P. Gimenez-Gomez, R. Escude-Pujol, C. Jimenez-Jorquera, M. Gutierrez-Capitan, Multisensor portable meter for environmental applications, *IEEE Sens. J.* 15 (2015) 6517–6523, <https://doi.org/10.1109/JSEN.2015.2460011>.
- [29] M. Gutiérrez-Capitán, M. Brull-Fontserè, C. Jiménez-Jorquera, Organoleptic analysis of drinking water using an electronic tongue based on electrochemical microensors, *Sensors* 19 (2019) 1435, <https://doi.org/10.3390/S19061435>.
- [30] A.D. McNaught, A. Wilkinson, IUPAC, Blackwell Scientific Publications, Oxford, 1997 <https://doi.org/10.1351/goldbook>.
- [31] M. Gutierrez, A. Llobera, J. Vila-Planas, F. Capdevila, S. Demming, S. Büttgenbach, S. Minguez, C. Jimenez-Jorquera, Hybrid electronic tongue based on optical and electrochemical microensors for quality control of wine, *Analyst* 135 (2010) 1718–1725, <https://doi.org/10.1039/c0an00004c>.
- [32] P. Giménez-Gómez, R. Escudé-Pujol, F. Capdevila, A. Puig-Pujol, C. Jiménez-Jorquera, M. Gutiérrez-Capitán, Portable electronic tongue based on microensors for the analysis of cava wines, *Sensors* 16 (2016), <https://doi.org/10.3390/s16111796>.
- [33] A. Cazalé, W. Sant, J. Launay, F. Ginot, P. Temple-Boyer, Study of field effect transistors for the sodium ion detection using fluoropolysiloxane-based sensitive layers, *Sens. Actuators B Chem.* 177 (2013) 515–521, <https://doi.org/10.1016/J.SNB.2012.11.054>.
- [34] A.R.L. Fraga, J.C. Quintana, G.L. Destri, N. Giambanco, R.G. Toro, F. Punzo, Polymeric membranes conditioning for sensors applications: Mechanism and influence on analytes detection, *J. Solid State Electrochem.* 16 (2012) 901–909, <https://doi.org/10.1007/s10008-011-1456-y>.
- [35] M. Guzinski, J.M. Jarvis, B.D. Pendley, E. Lindner, Equilibration time of solid contact ion-selective electrodes, *Anal. Chem.* 87 (2015) 6654–6659, <https://doi.org/10.1021/acs.analchem.5b00775>.
- [36] J.M. Margarit-Taulé, M. Martín-Ezquerro, R. Escudé-Pujol, C. Jiménez-Jorquera, S.-C. Liu, Cross-compensation of FET sensor drift and matrix effects in the industrial continuous monitoring of ion concentrations, *Sens. Actuators B Chem.* 353 (2022), 131123, <https://doi.org/10.1016/J.SNB.2021.131123>.
- [37] H.-M. Sheu, S.-C. Chao, T.-W. Wong, J. Yu-Yun, J.-C. Tsai, Human skin surface lipid film: an ultrastructural study and interaction with corneocytes and intercellular lipid lamellae of the stratum corneum, *Br. J. Dermatol.* 140 (1999) 385–391, <https://doi.org/10.1046/j.1365-2133.1999.02697.x>.
- [38] G. Dimeski, P. Mollee, A. Carter, Effects of hyperlipidemia on plasma sodium, potassium, and chloride measurements by an indirect ion-selective electrode measuring system, *Clin. Chem.* 52 (2006) 155–156, <https://doi.org/10.1373/CLINCHEM.2005.054981>.
- [39] S.K. Datta, P. Chopra, Interference in ion-selective electrodes due to proteins and lipids, *J. Appl. Lab. Med.* 7 (2022) 589–595, <https://doi.org/10.1093/JALM/JFAB125>.
- [40] E.D.B. Goulet, A. Asselin, J. Gosselin, L.B. Baker, Measurement of sodium concentration in sweat samples: comparison of five analytical techniques, *Appl. Physiol. Nutr. Metab.* 42 (2017) 861–868, <https://doi.org/10.1139/apnm-2017-0059>.
- [41] E.D.B. Goulet, T. Dion, É. Myette-Côté, Validity and reliability of the Horiba C-122 compact sodium analyzer in sweat samples of athletes, *Eur. J. Appl. Physiol.* 112 (2012) 3479–3485, <https://doi.org/10.1007/s00421-012-2331-y>.
- [42] M. Rovira, C. Fernández-Sánchez, S. Demuru, P. Kunnel Brince, D. Briand, C. Jimenez-Jorquera, Multisensing wearable technology for sweat biomonitoring, *Eng. Proc.* 6 (2021) 78, <https://doi.org/10.3390/43S2021Dresden10113>.
- [43] C. Lafaye, M. Rovira, S. Demuru, S. Wang, J. Kim, B.P. Kunnel, C. Besson, C. Fernandez-Sanchez, F. Serra-Graells, J.M. Margarit-Taule, J. Aymerich, J. Cuenca, I. Kiselev, V. Gremaux, M. Saubade, C. Jimenez-Jorquera, D. Briand, S.C. Liu, Real-time smart multisensing wearable platform for monitoring sweat biomarkers during exercise, *BioCAS 2022 - IEEE Biomed. Circuits Syst. Conf. Intell. Biomed. Syst. A Better Futur. Proc.* (2022) 173–177, <https://doi.org/10.1109/BIOCA54905.2022.9948565>.
- [44] N. LeBou, B. Rueckauer, P. Sun, M. Rovira, C. Jiménez-Jorquera, S.C. Liu, J. M. Margarit-Taulé, Real-time edge neuromorphic tasting from chemical microsensor arrays, *Front. Neurosci.* 15 (2021) <https://doi.org/10.3389/fnins.2021.771480>.

**Meritxell Rovira** received her M. Sc. Degree in Analytical Chemistry from the Universitat de Barcelona, Spain, in 2018. Then, she joined the Chemical Transducers Group (GTQ) at the Instituto de Microelectrónica de Barcelona, IMB-CNM, CSIC, as a Predoctoral Fellow. The aim of her doctoral thesis is to develop a platform that enables the continuous and real-time monitoring of biomarkers in sweat during the performance of a physical activity. Her main research interest is the application of (bio)chemical sensors to clinical and biomedical analysis.

**Celine Lafaye** received her B. Sc. Degree in Biosciences Engineering from INSA, Lyon, France in 2005 and her PhD in Protein Biochemistry from University of Grenoble Alps in 2009. She collaborated on several research projects on Proteins biochemistry and crystallography in European laboratories in Brussels and Grenoble. She has been working since 2018 as a post-doc researcher in the WeCare project, granted by the Swiss National Science Foundation in the sports medicine team at CHUV (Lausanne) to study sweat composition during exercise. In parallel with her professional career, she practices mountain running at national level (French trail running champion 2013 and 2016).

**Shu Wang** received her M.Sc. degree in Biomedical Engineering from ETH Zurich, Zurich, Switzerland, in 2018. Since then, she has been a doctoral student at the Institute of Neuroinformatics, University of Zurich and ETH Zurich. Her current research interests include deep learning algorithms for the analysis and prediction of time series, in particular biosignals.

**César-Fernández-Sánchez** is Scientific Researcher of CSIC and Head of the Chemical Transducers Group at IMB-CNM (CSIC). He holds a BSc in Analytical Chemistry and PhD in Chemistry, from the University of Oviedo (Spain). He did a short postdoctoral stay at Universidade do Minho (Portugal) before being awarded a Marie Curie Individual Fellowship hosted at Newcastle University (UK) to work on impedance-based biosensors for the detection of cancer biomarkers. His current research interests are on the implementation of robust miniaturized electrochemical sensors in compact analytical platforms



that could be mass-produced and deployed for in-situ detection of target chemical parameters in liquids and with the aim of transferring them to the market.

**Mathieu Saubade** earned his medical degree from the Free University of Brussels in 2008 and completed his residency training in Switzerland. He is specialist in physical and rehabilitation medicine, and graduated in sports and exercise medicine since 2014. He is currently attending physician at the Swiss Olympic Medical Center of the University Hospital of Lausanne, and at the department of health promotion and prevention at Unisanté, Lausanne. He is member of the WeCare research project, granted by the Swiss National Science Foundation (2018–2022), and doing a PhD in life sciences at the University of Lausanne, working on the effects of dehydration on sweat physiology and other biological parameters during exercise

**Shih-Chii Liu** received her Ph.D. degree in Computation and Neural Systems from the California Institute of Technology, Pasadena, in 1997. She is currently an Adjunct Professor in the Faculty of Science at the University of Zurich. She co-directs the Sensors

Group at the Institute of Neuroinformatics, University of Zurich, Switzerland and is an IEEE Fellow. Her research interests include low-power neuromorphic event-driven sensor design; bio-inspired deep learning algorithms and hardware for energy-efficient, real-time, adaptive intelligent systems.

**Cecilia Jimenez** received her Ph.D. degree in Chemistry from the Autonomous University of Barcelona, Spain, in 1993. She is currently Research Scientist at the Instituto de Microelectronica de Barcelona IMB-CNM, CSIC, Spain. She was the director of the Chemical Transducer Group (GTQ) at the IMB-CNM from January 2003 to June 2013 and deputy director of the IMB-CNM from July 2019 to July 2021. She is specialist in the development of integrated analytical systems and Point of care devices based on (bio) chemical sensors -electrochemical semiconductor-based sensors based on ISFETs (Ion selective Field Effect Transistors), metal thin film microelectrodes, microelectrode arrays (UMEAs) and interdigitated electrodes- and their application to environmental control, food industrial processes monitoring, clinical and biomedical analysis.